

1 Antibody effector functions are required for broad and potent protection of neonates from herpes
2 simplex virus infection

3

4 Matthew D. Slein^{1, 2#}, Iara M. Backes^{1, 2#}, Callaghan R. Garland¹, Natasha S. Kelkar^{1, 2}, David A.
5 Leib^{1*} & Margaret E. Ackerman^{1, 2, 3*}

6

7 # Authors contributed equally

8 *Corresponding authors

9 ¹Department of Microbiology and Immunology, Geisel School of Medicine at Dartmouth,
10 Lebanon, NH 03756, USA.

11 ²Thayer School of Engineering, Dartmouth College, Hanover, NH 03755, USA.

12 ³Lead Contact

13 *Correspondence: David.a.leib@dartmouth.edu, Margaret.e.ackerman@dartmouth.edu

14 **Summary**

15 The failure of multiple herpes simplex virus (HSV) vaccine candidates that induce
16 neutralizing antibody responses raises the hypothesis that other activities, such as Fc domain-
17 dependent effector functions, may be critical for protection. While neonatal HSV (nHSV)
18 infection result in mortality and lifelong neurological morbidity in humans, it is uncommon among
19 neonates with a seropositive birthing parent, suggesting the potential efficacy of antibody-based
20 therapeutics to protect neonates. We therefore investigated the mechanisms of monoclonal
21 antibody (mAb)-mediated protection in a mouse model of nHSV infection. Both neutralization
22 and effector functions contributed to robust protection against nHSV-1. In contrast, effector
23 functions alone were sufficient to protect against nHSV-2, exposing a functional dichotomy
24 between virus types that is consistent with vaccine trial results. Together, these results
25 emphasize that effector functions are crucial for optimal mAb-mediated protection, informing
26 effective Ab and vaccine design, and demonstrating the potential of polyfunctional Abs as potent
27 therapeutics for nHSV infections.

28
29

30 **Keywords:**

31

32 antibody engineering, Fc effector functions, neonatal HSV infections, neutralizing antibody,
33 monoclonal antibody therapeutics

34 Introduction

35 When encountered during the neonatal period, herpes simplex virus (HSV) infections
36 can result in loss of life or long-term neurological disability¹⁻³. Neonatal infections can present as
37 skin, eye, and mouth (SEM) disease, which is amenable to antiviral therapy, or more invasive
38 disseminated and/or central nervous system (CNS) disease. While new treatment regimens with
39 acyclovir and its derivatives have improved outcomes, mortality following disseminated disease
40 remains unacceptably high^{4,5}. Most neonatal HSV (nHSV) infections are vertically transmitted
41 during birth from a recently infected birthing parent who has not yet developed a mature
42 antibody response to HSV type 1 or type 2 (HSV-1, HSV-2)⁶. Given the severity of neonatal
43 infection resulting from primary maternal infection^{6,7}, birthing parent seropositivity is believed to
44 be protective due to the transfer of HSV-specific antibodies (Abs) via the placenta^{2,5,8}. High titers
45 of neutralizing or antibody-dependent cellular cytotoxicity (ADCC)-inducing Abs in infected
46 neonates have been associated with less severe disease^{9,10}. Animal studies support the notion
47 that neutralization and Fc-effector functions, such as ADCC, antibody-dependent cellular
48 phagocytosis (ADCP), and antibody-dependent complement deposition (ADCD) can aid in the
49 clearance of acute HSV infection¹¹⁻¹⁴. Further insights into how antibodies exert direct and
50 indirect antiviral activities to protect against infection could aid in the design of both passive and
51 active immunization strategies for HSV.

52 To this end, whether neutralization or effector functions play a dominant role in
53 protection from HSV-mediated disease has long been unclear, as conflicting results have been
54 reported in animal models^{12,13,15-17}. Previous studies differentiated effector functions from
55 neutralization by treating with digested antibody (Fab) fragments¹⁸. However, digestion is known
56 to compromise neutralization potency and half-life, which confounds interpretation of study
57 results. Other studies have sought to answer this question using polyclonal Ab or mAbs that
58 could either neutralize or carry out specific effector functions^{10,19}. While such approaches have
59 contributed to our understanding of the potential contributions of Ab effector functions,

60 disparities in protection from disease could also be attributed to the specific epitope(s) targeted,
61 differences in Ab affinity or avidity, or other factors. Ab Fc engineering strategies that allow
62 separation of Fc-dependent effector functions from neutralization provide a platform to improve
63 experimental resolution in defining Ab-dependent mechanisms of protection^{20–23}, which can
64 inform both vaccine design and therapeutic mAb development.

65 Like other consequential early life pathogens, most studies of HSV have focused on
66 adult animal models. There is therefore a dearth of information on how Abs protect in the
67 neonatal period. Given this knowledge gap, we sought to investigate the mechanism(s) by
68 which Abs that target glycoprotein D (gD) mediate protection against nHSV-1 and nHSV-2
69 infections. Using a mouse model of nHSV infection, we demonstrate that there are distinct
70 mechanisms of Ab-mediated protection that differ between viral types, motivating the
71 optimization of Ab therapeutics that could ameliorate nHSV. Given the short time window of
72 vulnerability to nHSV, this work could facilitate the design of effective therapeutic mAbs, whose
73 timely administration could yield tremendous benefit for this devastating disease.

74

75 Results

76 *Characterization of HSV-glycoprotein D (gD) specific monoclonal antibodies*

77 The mAbs used in this study protect both adult and neonatal mice from HSV-1- and
78 HSV-2-induced mortality^{14,24–26}, but the mechanisms by which they elicit protection have not
79 been defined. In order to better understand the contribution of neutralization and other Fc-
80 mediated functions, we studied UB-621, HSV8, and CH42 AAA, mAbs which exhibit different
81 neutralization potencies and effector function activity (**Figure 1A, Table S1**). To probe the
82 contributions of effector functions *in vivo*, HSV8 and CH42 AAA were expressed with Fc domain
83 point mutations that serve as functional FcγR and C1q binding knock outs (KO). UB-621 and
84 HSV8 are unmodified human IgG1 mAbs, while CH42 AAA has been engineered with

85 S298A/E333A/K334A mutations, which increase affinity for FcγRIIIA²⁷. For construction of KO
86 mAbs, we incorporated LALA PG²⁸ mutations into HSV8 and the N297A²⁹ substitution into
87 CH42. VRC01³⁰, an HIV-specific IgG1 mAb was included as an isotype control. The Fc receptor
88 (FcR) binding profiles of the engineered mAbs were evaluated *in vitro* (**Figure 1B, Figure S1**).
89 The binding patterns of all three Fc-intact antibodies, UB-621, HSV8, and CH42 AAA were
90 comparable, with CH42 AAA exhibiting the strongest binding to all human and mouse FcRs
91 tested. As expected, the HSV8 LALA PG variant displayed diminished binding to both human
92 and mouse FcRs as compared to HSV8. The CH42 NA variant also exhibited diminished
93 binding to human and mouse FcRs, with the exception of murine FcγRI, to which binding was
94 only slightly diminished. Importantly, given our use of these mAbs in mouse experiments, the
95 Fc-modified and -unmodified forms of each HSV-specific mAb displayed comparable binding
96 profiles to the four mouse FcR as to their human counterparts. These data indicate a high level
97 of concordance between species.

98 To more directly assess the function of each mAb, *in vitro* assays of antigen recognition,
99 neutralization, and effector function were performed (**Figure 2**). Each HSV-specific mAb bound
100 to both recombinantly expressed gD and gD expressed on the surface of mammalian cells
101 (**Figure 2A-B, Figure S2B**). In contrast, the isotype control, VRC01, showed no binding.
102 Notably, while CH42, HSV8, and UB-621 exhibited different antigen binding dose-response
103 profiles from each other, the binding of Fc KO forms of HSV8 and CH42 to antigen were
104 unchanged. Furthermore, direct antiviral activity afforded by antigen recognition again varied by
105 mAb, but not by Fc modification (**Figure 2C-D**). UB-621 and HSV8 potently neutralized both
106 HSV-1 and HSV-2, while CH42 poorly neutralized both viruses. Consistent binding and
107 neutralization activities of unmodified and Fc KO mAbs permits the isolation of Fab- from Fc-
108 dependent activities.

109 Lastly, we tested the *in vitro* effector functions of these mAbs. We profiled their ability to
110 promote FcγRIIIA activation upon recognition of recombinant or cell-expressed gD as a

111 surrogate for ADCC activity (**Figure 2E-F**). We also measured their ability to induce
112 complement deposition and phagocytosis (**Figure 2G-H, Figure S2A, C**). HSV8, UB-621, and
113 CH42 AAA all elicited effector functions *in vitro*, whereas KO mAbs were unable to elicit
114 FcγRIIIA activation, complement deposition, or phagocytosis. As may have been anticipated
115 from stronger binding to FcγRIIIA and FcγRIIA, CH42 AAA exhibited the most potent ADCC and
116 phagocytic activity, indicating that the AAA mutations enhanced the ability of CH42 to elicit Fc
117 function. CH42 NA, which eliminates the conserved Fc-glycan, did maintain some phagocytic
118 activity, presumably due to residual binding to human FcγRI. Consistent with this observation,
119 others have reported that aglycosylated IgG1 mAbs retain phagocytic activity via FcγRI
120 expressed on macrophages^{31,32}. Taken together, these experiments demonstrated the divergent
121 activities of the mAb panel, supporting its utility to defining *in vivo* mechanisms of action.

122

123 *Neutralization and Fc-mediated functions contribute to nHSV survival.*

124 To begin to understand the roles of viral neutralization and Fc effector functions in
125 mediating protection against a neonatal HSV challenge, 2-day old C57BL/6J pups were given
126 intraperitoneal (i.p.) injections with 40 μg mAb, then immediately challenged with 1.0 x 10⁴ PFU
127 HSV-1 intranasally (i.n.). Pups that received potently neutralizing mAbs HSV8 or UB-621 had
128 improved survival as compared to pups that received non-neutralizing mAb (CH42 AAA)
129 (**Figure 3A-B**). That said, all three HSV-specific antibodies improved survival as compared to
130 isotype control (VRC01) (**Figure 3A-C**). HSV-infected mice treated with CH42 NA, which lacks
131 both neutralization and effector function activity, succumbed to infection (**Figure 3B**). In
132 contrast, the mice that received the neutralizing but effector function KO HSV8 LALA PG,
133 survived HSV-1 infection (**Figure 3A**). These results indicate that for HSV8, neutralization alone
134 was sufficient to mediate protection, while the moderate protection mediated by CH42 AAA was
135 wholly Fc-dependent.

136 As an orthogonal test to define the specific contribution of Fc γ R-dependent Fc-effector
137 functions in mediating protection, Fc γ R-deficient mice (Fc γ R $^{-/-}$)³³ were treated i.p. with mAbs
138 and challenged i.n. with 1.0×10^4 PFU HSV-1. Fc γ R $^{-/-}$ mice that received neutralizing mAbs
139 HSV8, HSV8 LALA PG, and UB-621 exhibited increased survival as compared to CH42 AAA
140 and control IgG (**Figure 3D-F**). They were, however, considerably more susceptible to HSV
141 infection as compared to C57BL/6J wild type mice. Viral neutralization was highly protective in
142 WT mice but not in Fc γ R $^{-/-}$ mice, indicating a role for Fc function in contributing to protection
143 against HSV-1 in neonatal mice.

144

145 *Fc-functions are protective in the absence of complete viral neutralization*

146 Given the increased mortality observed in Fc γ R $^{-/-}$ mice treated with potentially neutralizing
147 mAbs, we next investigated the role of Fc-functions under conditions of maximal viral
148 neutralization. Achieving maximal neutralization activity was accomplished by pre-incubating
149 excess mAb with 1.0×10^4 PFU of HSV-1 prior to *in vivo* challenge. With this experimental
150 design, both C57BL/6J and Fc γ R $^{-/-}$ mice were completely protected from disease by HSV8 and
151 UB-621 (**Figure 4A, D**). In contrast, when virus was pre-incubated with 20 μ g of CH42 AAA, the
152 majority of the pups succumbed to infection (**Figure 4B**), as did all animals treated with the
153 isotype control mAb (**Figure 4C**). While increasing the CH42 AAA concentration fivefold to 100
154 μ g of mAb/pup did improve survival (**Figure 4B**), it was unable to achieve the complete
155 protection seen when mice were administered neutralizing mAbs. In contrast to neutralizing
156 mAbs, even a 100 μ g dose of CH42 AAA failed to protect Fc γ R $^{-/-}$ pups (**Figure 4E**), who
157 exhibited survival comparable to the isotype control mAb (**Figure 4F**). These results provide
158 evidence that Fc γ R-mediated activities are not necessary to provide protection in the context of
159 fully neutralized HSV-1 but can be responsible for protection in the absence of complete
160 neutralization.

161

162 *The relative impacts of neutralization and Fc-effector functions are mAb dose-dependent*

163 There was no difference in survival of pups treated with HSV8 or HSV8 LALA PG mAbs
164 at the 40 µg dose, and full protection of FcγR^{-/-} mice with neutralizing mAb-opsonized virus was
165 observed. Together, these data indicate the lack of a major role for Fc-effector functions in
166 mediating protection in the context of high levels of neutralizing activity. We wished, therefore,
167 to assess the hypothesis that Fc-effector functions may be more important at lower antibody
168 doses³⁴. To test this possibility, we treated C57BL/6J mice with 10 µg mAb delivered i.p. and
169 subsequently challenged with a lethal dose of HSV-1. As expected, this dose of HSV8 was less
170 protective than the 40 µg dose. However, this lower dose of HSV8 LALA PG was completely
171 unable to protect (**Figure 5A**), demonstrating that neutralization alone is insufficient to protect
172 mice at lower mAb doses. Intriguingly, CH42 AAA provided comparable protection to HSV8 at
173 the 10 µg dose (**Figure 5B**). In contrast, 10 µg of CH42 NA and the isotype control failed to
174 protect mice from HSV-mediated mortality (**Figure 5C**). Effector functions, therefore, mediate
175 protection from HSV-1-induced mortality at low antibody concentrations, at which viral
176 neutralization may be incomplete.

177 As an additional metric to explore the relative contributions of neutralization and effector
178 functions in mediating protection, we assessed viral titers in various organs following 10 µg mAb
179 treatment (**Figure 5 D-F**). At 5 days post infection, both HSV8 and CH42 AAA significantly
180 reduced viral burden in the brain, trigeminal ganglia (TG), and visceral organs (liver, spleen, and
181 lungs) as compared to the isotype control mAb. HSV8 LALA PG, however, only significantly
182 reduced viral burden in the brain as compared to isotype control (**Table S2**). The viral burden in
183 pups treated with CH42 NA was indistinguishable from pups given an isotype control mAb.
184 While not statistically significant, pups treated with HSV8 had lower viral burden as compared to
185 pups given HSV8 LALA PG, consistent with survival data in indicating a contribution of effector
186 functions in mediating protection (**Figure 5D**). Further evidence for the role of effector functions
187 in mediating protection was observed in the differences in viral burden in pups treated with

188 CH42 AAA and CH42 NA. Pups treated with CH42 AAA had statistically significantly lower viral
189 burden in the brain, TG, spleen, and lungs as compared to mice given CH42 NA (**Figure 5E**). Of
190 note, some pups given HSV8 LALA PG, CH42 NA, or the isotype control died prior to day 5 post
191 infection, while no pups given HSV8 or CH42 AAA died prior to organ collection. Taken
192 together, these data support a role for effector functions in protecting mice from HSV-1
193 mediated mortality and viral burden in the nervous system and viral dissemination.

194

195 *HSV-specific mAbs require effector functions for control of viral replication.*

196 To determine whether effector functions contribute to viral clearance, mouse pups were
197 infected in a non-lethal challenge model utilizing a luciferase-producing recombinant HSV-1³⁵,
198 allowing real-time imaging of *in vivo* viral replication. Pups were challenged with HSV-1
199 17syn+dLux i.n., and were treated the following day with 10 µg of HSV8, HSV8 LALA PG, CH42
200 AAA, CH42 NA or an isotype control mAb delivered i.p.. Consistent with the results of survival
201 and viral load experiments, mice that received a 10 µg dose of either HSV8 LALA PG or CH42
202 NA exhibited significantly greater levels of viral replication as measured by bioluminescence
203 than mice treated with HSV8 or CH42 AAA starting at day 4 post infection (**Figure 6A-B**).
204 Bioluminescence in Fc KO mAb-treated mice persisted for significantly longer than in those that
205 received mAbs with intact effector functions and was comparable to the animals that received
206 the IgG control mAb (**Figure 6A-B**). Statistically significant differences in bioluminescence
207 were observed in animals treated with Fc KO versus Fc-functional mAbs (**Figure 6C**). Given the
208 equivalent neutralization profiles of HSV8 and HSV8 LALA PG, differences in viral replication
209 and dissemination must be attributable to the lack of effector functions in the LALA PG variant.
210 Moreover, CH42 AAA, which does not neutralize, cleared virus significantly faster than its Fc KO
211 counterpart. These results extend observations from the lethal challenge model and
212 demonstrate that effector functions contribute to control of HSV-1 replication.

213

214 *Antibody functions contributing to protection differ between HSV serotypes*

215 Since nHSV is caused by both HSV-1 and HSV-2, we next sought to examine whether
216 the mechanism and patterns of protection were equivalent for both viruses. To test mechanism
217 of protection against HSV-2, two-day old C57BL/6J mouse pups were treated with 40 µg of
218 HSV-specific mAb or isotype control and then challenged with 300 PFU of HSV-2 strain G³⁶. In
219 contrast to HSV-1, and despite differences in neutralizing activities, both HSV8 and CH42 AAA
220 provided equivalent protection against lethal challenge with HSV-2 (**Figure 7A,B**). Moreover,
221 the Fc mutations in HSV8 LALA PG and CH42 NA completely ablated their protective activities,
222 rendering them equivalent to the isotype control mAb (**Figure 7A-C**). These results demonstrate
223 that Fc-mediated effector functions, and not viral neutralization, are essential for protection
224 against HSV-2 infection, exposing a dichotomy between viral subtypes. Together, these data
225 demonstrate that optimal antibody-mediated protection against HSV-1 in neonates is achieved
226 by both neutralization and effector functions. In contrast, for protection against HSV-2, effector
227 functions alone are sufficient.

228

229 **Discussion**

230 Understanding the mechanism by which antibodies provide protection has the potential
231 to contribute to the development of mAb-based prevention and therapy, as well as to inform
232 vaccine design. In this study, nHSV clinical outcomes depended on mAb specificity,
233 neutralization potency, effector functions, dose, and viral strain. Both neutralization and effector
234 functions improved virological outcomes following HSV-1 challenge. At higher Ab doses,
235 neutralizing mAbs afforded near-complete protection, whereas the non-neutralizing mAb
236 afforded only moderate protection, which was Fc-dependent since CH42 NA failed to prevent
237 mortality. In contrast, under the same mAb dose and challenge conditions, viral neutralization
238 alone was unable to prevent significant mortality in FcγR^{-/-} mice. Notably, pre-incubating the

239 virus with neutralizing mAb prior to challenging FcyR^{-/-} mice completely protected these mice
240 from mortality. This apparent discrepancy in the protective contribution of Fc-dependent
241 antibody functions observed with KO mAbs versus FcyR^{-/-} mice could be attributed to, for
242 example, residual mAb effector function, differences in antibody biodistribution, and the intrinsic
243 susceptibility of FcyR^{-/-} mice²⁰, among other factors.

244 When mAb was present at low concentrations, effector functions were more protective
245 than viral neutralization. In contrast, when present at high levels systemically, or when pre-
246 incubation with virus before nasal challenge, neutralization activity was the principal mechanism
247 of action. This functional shift suggests that antibody concentration and biodistribution are
248 determinants of the dominant mechanism of protection. Our findings support the hypothesis that
249 antibody-mediated protection against HSV-1 is driven primarily by neutralization at high doses,
250 while at lower doses both neutralization and Fc-effector functions play a role, as has been
251 previously hypothesized³⁴. Evidence in support of this hypothesis has been seen for other
252 viruses. At sub-neutralizing antibody doses, mAb effector functions can be associated with
253 improved resistance to infection^{37,38}, control of viremia^{39,40}, and clearance of virions⁴¹ during
254 SHIV infection in non-human primates. Additionally, optimal mAb-mediated protection against
255 SARS-CoV-2 infection required effector functions in addition to viral neutralization, particularly
256 when neutralization potency was compromised⁴²⁻⁴⁴. Although these viruses differ from HSV in
257 their pathogenesis and immune evasion strategies, our data support the idea that mAb dose is a
258 pivotal determinant of the mechanism of protection. Antibody dose, however, can also directly
259 impact clinical outcome in terms of viral pathogenesis. Sub-neutralizing doses of antibodies
260 against Dengue virus can lead to FcR-driven antibody-dependent enhancement of disease⁴⁵,
261 furthering the consideration of antibody dose as a determinant for mechanism of action.

262 Given the ability of HSV8 LALA PG to protect against HSV-1, its relative inability to
263 protect against HSV-2 was unexpected. The inability of both CH42 NA and HSV8 LALA PG to
264 protect against HSV-2 indicates that Fc-mediated effector functions and not viral neutralization

265 drive mAb-mediated protection against this serotype. This result may explain in part the failures
266 of human HSV-2 vaccine trials⁴⁶⁻⁴⁸. A subunit vaccine containing gD and gB that induced high
267 titers of neutralizing antibodies but low titers of ADCC-inducing antibodies⁴⁹ showed poor
268 efficacy⁵⁰, indicating that neutralizing activity was not sufficient for prevention of genital disease
269 and transmission of HSV-2. Similarly, a later gD subunit vaccine candidate that induced robust
270 neutralizing titers but little to no ADCC activity⁵¹ had 58% efficacy in preventing HSV-1 genital
271 disease, but could not prevent HSV-2 genital disease⁴⁶. In this trial, neutralization titers against
272 HSV-2 did not correlate with protection and could not explain the lack of vaccine efficacy⁵².
273 Overall, the lack of protection afforded by neutralization and the poor effector function of
274 antibodies raised by these vaccine candidates are consistent with the hypothesis that protection
275 against HSV-2 requires effector functions. In our study, protection against HSV-2-mediated
276 mortality was independent of mAb neutralization potency in that CH42 AAA poorly neutralized
277 HSV-2 and yet provided protection comparable to HSV8. Consistent with this result, a non-
278 neutralizing but FcγR-activating mAb that targets gB mediated protection from HSV-2 *in vivo*⁵³.

279 The importance of antibody effector functions was also observed in bioluminescent
280 imaging experiments that sought to quantify viral load. Effector functions played the largest role
281 in contributing to viral control, as both HSV8 and CH42 AAA cleared the HSV-derived
282 bioluminescence significantly faster than their KO equivalents. Moreover, the ability for an
283 antibody to elicit effector functions also greatly contributed to the control of viral burden and viral
284 dissemination. Pups that received HSV8 or CH42 AAA had lower viral burden in tissues of the
285 nervous system and in visceral organs as compared to their functional KO counterparts. This
286 reduction in viral burden indicates a role for effector functions in the control of viral spread.
287 HSV8 LALA PG was also able to slightly reduce viral burden in the brain as compared to the
288 isotype control, indicating that neutralization still contributes to protection. Together, these
289 preclinical studies highlight the importance of investigating non-neutralizing antibody functions in
290 mediating protection against HSV disease, particularly HSV-2.

291 While there are caveats to direct translation of observations from animal models to
292 humans, prior studies provide a high degree of confidence as to which murine FcγR are
293 engaged when introducing human IgG1 into a mouse^{22,54}. The distribution of FcRs varies
294 between human and murine innate immune cells, but the overall effector functions elicited by
295 the differing cell types are conserved. ADCC activity elicited via human cells is generally a good
296 predictor of murine ADCC (predominantly carried out by macrophages and PMNs)⁵⁵. We
297 focused on mAbs specific for gD and tested a limited number of viral strains in a single mouse
298 strain background, and our results may or may not generalize across other target antigens,
299 mAbs, viruses, or host genetic backgrounds. Other caveats include when and where mAbs
300 initially encounter virus, particularly in the context of differing hosts. Given that humans show a
301 spectrum of anatomical, physiological, and immunological profiles, and based on the data of this
302 study, antibodies with broad functional activities are more likely to afford clinical efficacy. This
303 idea is supported by clinical evidence: both neutralizing and ADCC Ab activity serve as
304 biomarkers for protection of infants from disseminated HSV disease¹⁰. The inability of
305 neutralizing activity to serve as a reliable biomarker of vaccine-mediated protection in adults,
306 particularly for HSV-2, are also consistent with our results. Collectively, these data support the
307 conclusion that polyfunctional mAbs able to elicit both neutralization and effector functions are
308 the best candidates for therapeutic and prophylactic translation. Expanding the focus of vaccine
309 research and development to include activities beyond viral neutralization has the potential to
310 accelerate the quest for interventions to reduce the global burden of HSV infection.

311

312 Acknowledgments

313 We would like to thank all members of the Ackerman and Leib laboratories for their invaluable
314 help with critical discussion and scientific advice. We thank United BioPharma for providing UB-
315 621 and ZabBio for providing HSV8. The authors acknowledge the following Shared Resources
316 facilities: Irradiation, Pre-clinical Imaging and Microscopy Resource (IPIMSR) at the Norris
317 Cotton Cancer Center at Dartmouth with NCI Cancer Center Support Grant 5P30 CA023108-37.
318 These studies were partially supported by National Institutes of Health grants, NEI
319 5R01EY009083-28 to DAL, NIAID grants 5P01AI098681-08 and 5R21AI147714-02 to DAL,
320 U19AI145825 to MEA, R01AI176646 to DAL and MEA, and T32AI007363 to MDS.

321

322 Author Contributions

323 IMB, MDS, DAL, and MEA conceptualized the study. IMB, MDS, NSK, and CRG performed
324 experiments. DAL and MEA obtained funding and supervised research. IMB and MDS drafted
325 manuscript and generated figures. IMB, MDS, DAL, and MEA finalized manuscript and all other
326 authors have read and edited.

327

328 Declaration of Interests

329 IMB, DAL, and MEA report a patent WO2020077119A1 for mAbs used in this manuscript as a
330 method for the treatment for nHSV infections.

331 **Methods**

332 **RESOURCE AVAILABILITY**

333 **Lead Contact**

334 Further information and requests for reagents and resources should be directed to and will be
335 fulfilled by the lead contact Dr. Margaret E. Ackerman (margaret.e.ackerman@dartmouth.edu)

336

337 **Materials Availability**

338 Antibodies, cell lines, and plasmids generated for this study may be requested with a material
339 transfer agreement.

340

341 **Data and code availability**

342 All data reported in this paper will be shared by the lead contact upon reasonable request.

343 This paper does not report original code.

344 Any additional information required to reanalyze the data reported in this paper is available from
345 the lead contact upon request.

346

347 **EXPERIMENTAL MODEL AND STUDY PARTICIPANT DETAILS**

348 **Cell Lines**

349 Vero Cells (CCL-81) were purchased from American Type Culture Collection (ATCC) and were
350 maintained in Dulbecco's Modified Eagle's Medium (DMEM) containing 5% fetal bovine serum
351 (FBS) and 1% penicillin/streptomycin at 37°C with 5% CO₂. HEK293Ts were purchased from
352 ATCC and maintained in DMEM with 10% FBS at 37°C and 5% CO₂. The human monocytic cell
353 line, THP-1, was purchased from ATCC and maintained in RPMI-1640 supplemented with 10%
354 FBS and 55µM beta-mercaptoethanol at 37°C with 5% CO₂. EXPI293Fs were purchased from
355 ThermoFisher and were maintained in Expi293F Media (Thermo Fisher). Cells were grown in a

356 Thermo Scientific reach-in CO₂ incubator at 37°C with 8% CO₂ on an innOva 2300 platform
357 shaker at 125 RPM. Jurkat-Lucia NFAT CD16 cells were purchased from Invivogen and grown
358 in RPMI-1640 supplemented with 10% fetal bovine serum, 1 mM sodium pyruvate, 1x non-
359 essential amino acids, 1x penicillin/streptomycin, 100 µg/mL Normocin, 100 µg/mL Zeocin, and
360 10 µg/mL Blasticidin.

361

362 **Animals**

363 Naïve male and female C57BL/6J (RRID: IMSR_JAX:000664) were either purchased from The
364 Jackson Laboratories or bred in animal facilities at Dartmouth College in accordance with
365 institutional animal care and use committee protocols (Dartmouth College IACUC 2151).
366 C57BL/6J mice were bred according to IACUC protocols and 2-day-old offspring of both sexes
367 were then used in challenge studies. Naïve male and female B6.129P2-Fcγ1gtm1Rav N12
368 (FcγR^{-/-}) (model: 583) were purchased from Taconic Labs. FcγR^{-/-} mice were bred in
369 accordance with IACUC protocols and 2-day-old offspring of both sexes were used in challenge
370 studies.

371

372 **METHOD DETAILS**

373 *Mouse procedures and viral challenge.* C57BL/6J (B6) mice were purchased from The Jackson
374 Laboratory. FcγR^{-/-} mice (B6.129P2-Fcγ1gtm1Rav N12) were purchased from Taconic Labs³³.
375 Administration of mAbs was via the peritoneal route with a 25 µL Hamilton syringe in a 20 µL
376 volume under 1% isoflurane anesthesia. The wild-type viral strains used in this study were HSV-
377 1 17syn⁺⁵⁶, HSV-2 G (kindly provided by Dr. David Knipe)³⁶. The bioluminescent luciferase-
378 expressing recombinant virus HSV-1 17syn⁺/Dlux was constructed as previously described³⁵.
379 Viral stocks were prepared using Vero cells as previously described^{57,58}. Newborn pups were
380 infected i.n. on day 2 postpartum with indicated amounts of HSV in a volume of 5-10 µl under
381 1% isoflurane anesthesia. Pups were then monitored for survival, imaging, or viral burden

382 analysis. For survival studies, pups were challenged with 1×10^4 plaque forming units (PFU) of
383 HSV-1 (Strain 17), and 3×10^2 PFU of HSV-2 (Strain G), as indicated. Endpoints for survival
384 studies were defined as excessive morbidity (hunching, spasms, or paralysis) and/or >10%
385 weight loss (**Figures S3-5**). For bioluminescent detection, pups were injected i.p. with 20 μ l of
386 15 mg/mL D-luciferin potassium salt (Gold Biotechnology), placed in isoflurane chamber, and
387 moved into a Xenogen IVIS-200 with a warmed stage and continuous isoflurane. Pups were
388 typically imaged beginning at 1 day post-infection and serially imaged every day until 8 days
389 post-infection to monitor bioluminescence. For viral titers of organs, tissues were harvested 5
390 days post infection following cardiac perfusion with at least 5 mL of ice-cold PBS. All tissues
391 were collected in 1.7 mL tubes containing ~ 100 μ L of 1mm sterile glass beads and 1 mL of
392 DMEM containing 5% fetal bovine serum (FBS) and 1% penicillin/streptomycin. Tissue
393 homogenates were prepared via mechanical disruption using a Mini-Beadbeater-8 (BioSpec
394 Products). Organ titers were measured via plaque assay on Vero cells.

395
396 *Monoclonal antibodies.* CH42¹⁴ AAA plasmids were kindly provided by Dr. Anthony Moody
397 (Duke University). When expressed *in vitro*, CH42 contained the Fc mutation known as AAA
398 (S298A/E333A/K334A), which enhances antibody dependent cellular cytotoxicity²⁷. The variable
399 heavy chain sequence of CH42 was subcloned into a plasmid coded with an IgG1 heavy chain
400 backbone containing the N297A²⁹ mutation via QuikChange Site Directed Mutagenesis kit
401 (Agilent). Antibodies were expressed through co-transfection of heavy and light chain plasmids
402 in Expi293 HEK cells (Thermo Fisher) according to the manufacturer's instructions. Seven days
403 after transfection, cultures were spun at 3000 x g for 30 minutes to pellet the cells, and
404 supernatants were filtered (0.22 μ m). IgG was affinity purified using a custom packed 5 mL
405 protein A column with a retention time of 1 minute (ie. 5 mL/min) and eluted with 100 mM
406 glycine pH 3, which was immediately neutralized with 1 M Tris buffer pH 8. Eluate was then
407 concentrated to 2.5 mL for size exclusion chromatography on a HiPrep Sephacryl S-200 HR

408 column using an AktaPure FPLC at a flow rate of 1 mL/min of sterile PBS. Fractions containing
409 monomeric IgG were pooled and concentrated using spin columns (Amicon UFC903024) to
410 approximately 2 mg/mL of protein and either used within a week or aliquoted and frozen at -
411 80°C for later use. HSV8 mAb was kindly provided by ZabBio and Kentucky Bioprocessing, and
412 a clinical grade antibody preparation of UB-621 was kindly provided by United BioPharma.

413

414 *Measurement of antibody binding to mouse and human Fc Receptors*

415 Recombinant gD antigen⁵⁹, kindly provided by Dr. Gary Cohen (UPenn), was coupled to
416 MagPlex beads (Luminex) as previously described⁶⁰. gD mAbs were serially diluted in 1x PBS
417 with 0.1% bovine serum albumin (BSA) and 0.05% Tween-20 and incubated with antigen-
418 coupled beads overnight at 4°C with constant shaking. Beads were washed before being
419 incubated with recombinant biotinylated human Fc receptors⁶¹ (Duke Human Vaccine Institute)
420 or mouse Fc receptors (Sino Biologicals) that were tetramerized with streptavidin-PE for 1 hour.
421 The beads were washed and analyzed on the xMap system. The median fluorescence intensity
422 of at least 10 beads/region was recorded. An isotype control antibody and a buffer only control
423 were used to determine antigen-specific binding and assay background signal. Area under the
424 curve was calculated using Prism 9 (GraphPad).

425

426 *Viral Neutralization*

427 Serially diluted mAb and 50 PFU of HSV-1 st17 or HSV-2 G were incubated for 1 hour at 37°C
428 before being added to confluent Vero cells grown in 6 well plates. Immune complexes were
429 incubated with Vero cell monolayers for 1 hour at 37°C with 5% CO₂ with shaking every 15
430 minutes. Methylcellulose overlay was added to the wells after the hour incubation. Plates were
431 incubated for 48 (HSV-1) or 72 (HSV-2) hours at 37°C with 5% CO₂. Methylcellulose overlay
432 was removed, Vero cells were fixed with 1:1 ethanol:methanol before being stained with 12%
433 Giemsa overnight. Stain was removed and plaques were counted on a light box. Virus

434 neutralization (%) was calculated as [(# of plaques in virus only - # of plaques counted at mAb
435 dilution)/# of plaques in virus only well] x100.

436

437 *Antigen Binding ELISA*

438 The ability for the HSV-specific mAbs to bind to gD was evaluated via an ELISA. Briefly, the
439 wells of a high-binding 96 well plate were coated with 1 µg/mL gD in sodium bicarbonate buffer
440 pH 9.4 and incubated overnight at 4°C. The plates were washed 5x with 1x PBS, 0.1% BSA,
441 0.05% Tween-20 and blocked with 1x PBS with 2.5% BSA overnight at 4°C. The plates were
442 washed 5x. Antibodies were serially diluted in 1x PBS with 0.1% BSA over a seven point two-
443 fold dilution curve (10.66 nM – 0.16 nM), added to the plates, and incubated at room
444 temperature for 1 hour. The wells were washed 5x and incubated with 100 µl/well with an HRP-
445 conjugated anti-human IgG Fc antibody (1:10000 dilution, Invitrogen) for 1 hour. Wells were
446 washed a final time before being incubated with 100 µL/well 1-step Ultra TMB (Invitrogen) for 5
447 minutes. The reaction was halted with 100 µL/well 1N H₂SO₄. The plate was read at 450 nm on
448 a SpectraMax Paradigm Plate Reader (Molecular Devices). Buffer only wells were used as a
449 control and the assay was performed in technical replicate.

450

451 *Antibody-dependent cellular cytotoxicity (ADCC)*

452 A CD16 activation reporter assay was performed as previously described⁶². Briefly, the wells of
453 a high-binding 96 well plate were coated with 1 µg/mL recombinant gD protein in PBS and
454 incubated overnight at 4°C. The plate was washed 3x with 1x PBS with 0.01% Tween20 and
455 blocked at room temperature with 1x PBS with 2.5% BSA for 1 hour. Antibodies were serially
456 diluted in growth medium and added to the washed plate with 100,000 Jurkat Lucia NFAT CD16
457 cells/well (Invivogen). Antibodies and cells were incubated for 24 hours at 37°C with 5% CO₂. A
458 25 µL volume of the cell supernatant was removed and added to a new, opaque white 96 well
459 plate. A 75 µL volume of the QuantiLuc (Invivogen) substrate was added to the supernatant and

460 luminescence was immediately read on SpectraMax Paradigm plate reader (Molecular Devices)
461 using a 1 second integration time. A kinetic read time of 0, 2.5 and 5 minutes was performed,
462 and the reported values are the averages of the three reads. Buffer only wells were used as
463 negative controls and a cell stimulation cocktail with 2 µg/mL ionomycin was used as a positive
464 control. The assay was performed in technical replicate.

465

466 *Antibody-dependent cellular phagocytosis (ADCP)*

467 Antibody-dependent cellular phagocytosis was performed as previously described⁶³ with slight
468 modifications. Briefly, goat-anti human IgG F(ab')₂ (Invitrogen) was covalently coupled to
469 yellow-green carboxylate beads (Thermofisher). Antibodies were diluted in culture medium to a
470 starting concentration of 133 nM and serially diluted 4-fold 7 times. Diluted mAbs were
471 incubated with anti-human IgG beads for 2 hours at 37°C to form immune complexes. THP-1
472 (ATCC) cells (25,000/well) were added to the immune complexes and incubated at 37°C for 4
473 hours. Cells were washed 2x with cold 1x PBS prior to being fixed with 4% paraformaldehyde.
474 The cells were analyzed on a NovoCyte Advanteon flow cytometer (Agilent) (**Figure S2C**). A
475 phagocytosis score was calculated as the (percentage of FITC+ cells) x (the geometric mean
476 fluorescence intensity (gMFI) of the FITC+ cells)/100,000. Buffer only wells were used as
477 negative controls and the assay was performed in technical replicate with two biological
478 replicates.

479

480 *Engineering HEK293Ts expressing HSV-1 gD as a surface antigen:*

481 The gD gene was PCR amplified from HSV-1 strain 17 DNA. The gene was cloned into pLenti-
482 DsRed-IRES-EGFP vector (Addgene plasmid number 92194)⁶⁴ by restriction digestion using
483 Afe1 and BamH1 (New England BioLabs (NEB)). Restriction digestion was followed by ligation
484 using T4 DNA ligase (NEB). The ligated PCR product was transformed into NEB® Stable
485 Competent *E. coli* (High Efficiency). The gene insertion into the vector was confirmed by using

486 restriction digestion by SgrA1 (NEB) and plasmid sequencing (Azenta LifeSciences). The
487 sequence confirmed plasmid (transfer plasmid) and packaging vector (VSVG, PSPAX2) were
488 used at concentrations of 6 µg, 0.6 µg and 5.4 µg to transfect HEK293T cells at 60% confluency
489 in a T150 flask. Transfer plasmid and packaging vector were mixed with Opti-MEM
490 (ThermoFisher Scientific). In a separate tube, Opti-MEM and 109.38 µg Polyethylenimine (PEI)
491 was added. The DNA:Opti-MEM and PEI:Opti-MEM mixtures were combined and incubated
492 together for 15 min at room temperature prior to being added to the HEK-293Ts. Media was
493 replenished the next day (day 1). On day 2, the viral supernatant was collected and Lenti-X™
494 GoStix™ Plus (Takara) was used to test presence of lentiviral p24. The viral supernatant was
495 filtered using 0.45-micron filter and aliquots were stored at -80 °C.
496 Adherent HEK293T cells were trypsinized and 500,000 cells were mixed in 1 mL of thawed viral
497 supernatant, to which 0.8 µg of polybrene (Santa Cruz Biotechnology) was added. The mixture
498 was incubated in a 6 well plate at 37 °C, 5% CO₂. On the next day, old media was removed and
499 was replaced with 2 mL fresh media. At 4 days post transduction, GFP positive cells were
500 sorted using cell sorter (Sony Biotechnology, MA900) using a 100-micron sorting chip (Sony
501 Biotechnology) and cultured in media containing 1X penicillin/streptomycin. Non-transfected
502 HEK293T cells were used as a negative control to set the sort gates (**Figure S2**).

503
504 *Measurement of binding of antibody to HEK293Ts expressing HSV-1 gD as a surface antigen:*
505 HEK293T cells expressing HSV-1 gD as a surface antigen and non-transfected HEK293T cells
506 (control) were washed twice with PBS. Cells (200,000/well) were added to a 96 well V bottom
507 plate (USA Scientific). gD-specific antibodies were diluted to 20 µg/mL and serially diluted four-
508 fold in PBS + 1% BSA before being added to the cells. After a 1-hour incubation on ice, the cells
509 were washed twice with PBS + 1% BSA and stained with 10 µg/mL Alexa Fluor™ 647 Goat
510 anti-Human IgG (H+L) Cross-Adsorbed Secondary Antibody (ThermoFisher Scientific) diluted in

511 PBS with 1% BSA. After a 30 min incubation in the dark, cells were washed twice with PBS +
512 1% BSA and were resuspended in 100 μ L of PBS prior to fixation with 4% paraformaldehyde.
513 The antibody binding was measured by checking signal intensity of Alexa Fluor 647 using a
514 MACSQuant Analyzer (Miltenyi) (**Figure S2B**). The experiment had two biological replicates.
515 The data was analysed using FlowJo version 10.8.2.

516

517 *Antibody Dependent Complement Deposition:*

518 HEK293T cells expressing HSV gD as surface antigen and non-transfected HEK293T cells
519 (control) were washed twice with PBS. Cells (200,000/well) were added to a 96 well V bottom
520 plate (USA Scientific). Antibodies were diluted to 20 μ g/mL and serially diluted four-fold in PBS
521 + 1% BSA before being added to the cells. After 45 min, the cells were washed with PBS + 1%
522 BSA, followed by a wash with Gelatin Veronal Buffer (GVB++) (Complement Technology Inc).
523 Low-tox Guinea Pig complement (Cedarlane) was reconstituted in 1 mL cold distilled water, a
524 500 μ L volume of which was added to 9.5 mL GVB++. Diluted guinea pig complement (100 μ L)
525 was then added to each well prior to incubation with orbital shaking for 1 hour at 37 $^{\circ}$ C, with 5%
526 CO₂. The cells were then washed with PBS + 1% BSA prior to staining with 100 μ L of 1 μ g/mL
527 biotinylated goat anti-guinea pig C3 antibody (ICL labs) at room temperature for 1 hour. The
528 cells were washed twice with PBS + 1% BSA prior to addition of 100 μ L of 1 μ g/mL Streptavidin-
529 APC (ThermoFisher) and incubation for 1 hour at room temperature. After the incubation, the
530 cells were washed twice and resuspended in PBS + 1% BSA. Antibody-dependent activation of
531 complement protein C3 was measured using a MACSQuant Analyzer (Miltenyi) quantifying the
532 mean fluorescence intensity of APC (**Figure S2A**). The assay was performed with two biological
533 replicates. Heat-inactivated guinea pig complement was used as a control. For heat
534 inactivation, the serum was heated at 58 $^{\circ}$ C for 30 min. VRC01 antibody was used as a negative
535 control. The data was analysed using FlowJo version 10.8.2.

536

537 *CD16 activation assay (ADCC):*

538 HEK293T cells expressing HSV gD as surface antigen and non-transfected HEK293T cells
539 were washed 2x with PBS before being added to a V bottom plate (USA Scientific) (200,000
540 cells/well). Into the same plate, 100,000 cells/well of Jurkat Lucia NFAT CD16 cells (Invivogen)
541 were added, along with 180 μ L of assay media (RPMI 1640 + 10% FBS + 1mM sodium
542 pyruvate + non- essential amino acids + penicillin/streptomycin) and 20 μ L of diluted gD-specific
543 antibodies (in PBS + 1% BSA). The plate was incubated overnight at 37°C, 5% CO₂. After
544 overnight incubation, the cells were centrifuged and 25 μ L of supernatant was drawn from each
545 well and transferred into 96-well white walled clear bottom polystyrene plate (Costar) and mixed
546 with 75 μ L of reconstituted QUANTI-Luc™ reagent (InvivoGen). Luminescence was immediately
547 read on a SpectraMax Paradigm Plate reader (Molecular Devices) using 1s integration time.
548 Kinetic reads at 0 min, 2.5 min and 5 min were measured, and the mean reading was noted.
549 Cell Simulation Cocktail (eBioscience) was used as positive control. VRC01 was used as
550 negative control. The assay was performed with two biological replicates.

551

552 *Study Approval*

553 Procedures were performed in accordance with Dartmouth's Center for Comparative Medicine
554 and Research policies and following approval by the institutional animal care and use
555 committee.

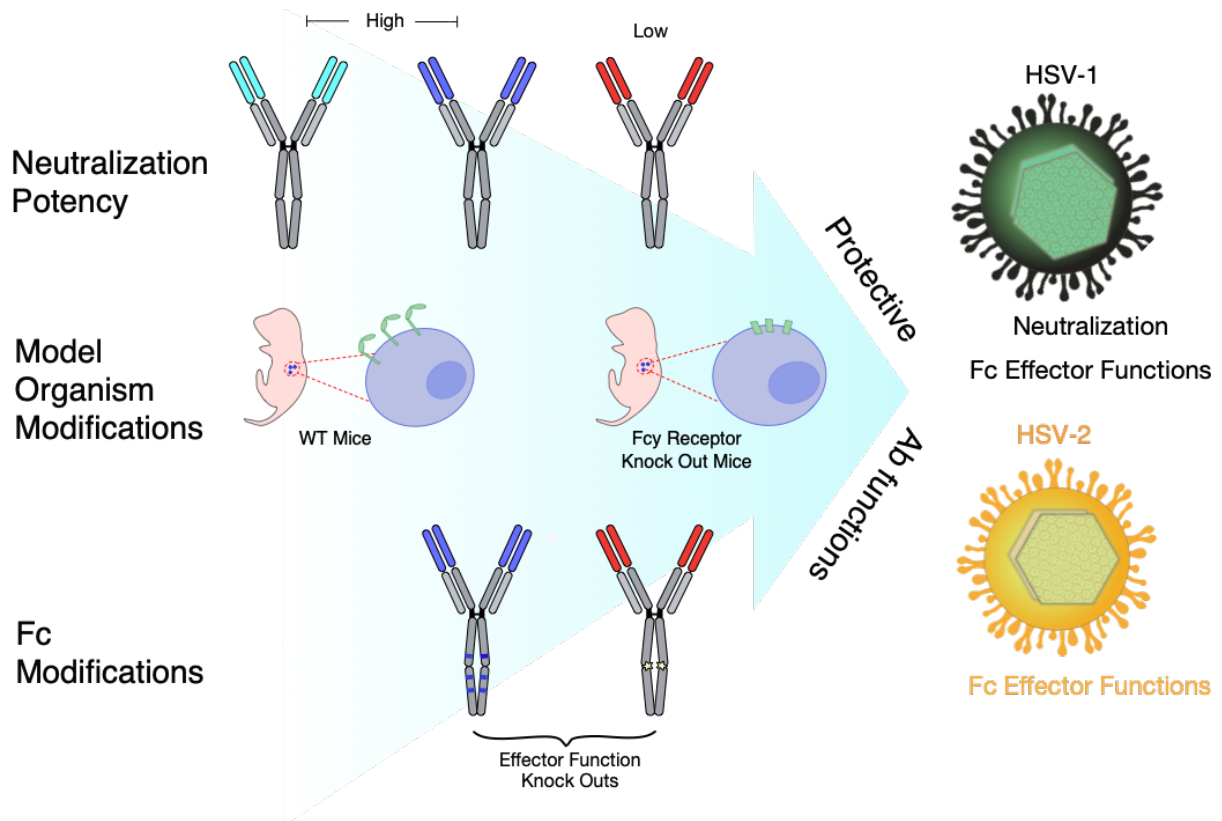
556

557 *Statistical Analysis*

558 Prism 9 (GraphPad) software was used for statistical tests. For survival studies, HSV-specific
559 mAbs were compared to isotype controls using the Log-rank Mantel-Cox test to determine p
560 values. HSV-specific Fc-competent and KO mAbs were also compared to each other using the

561 Log-rank Mantel-Cox test to determine p values. For imaging studies, groups and time points
562 were compared to each other via 2-way ANOVA, with Tukey's test for multiple comparisons to
563 determine p values. For viral burden analysis, mAbs were compared to each other within each
564 organ group via an ordinary 2-way ANOVA with Bonferoni's test for multiple comparison. Within
565 each organ, HSV-specific mAbs were compared to the isotype control mAb via a 2-way ANOVA
566 with Dunnet's test for multiple comparisons.

567 Figures, Tables and Legends

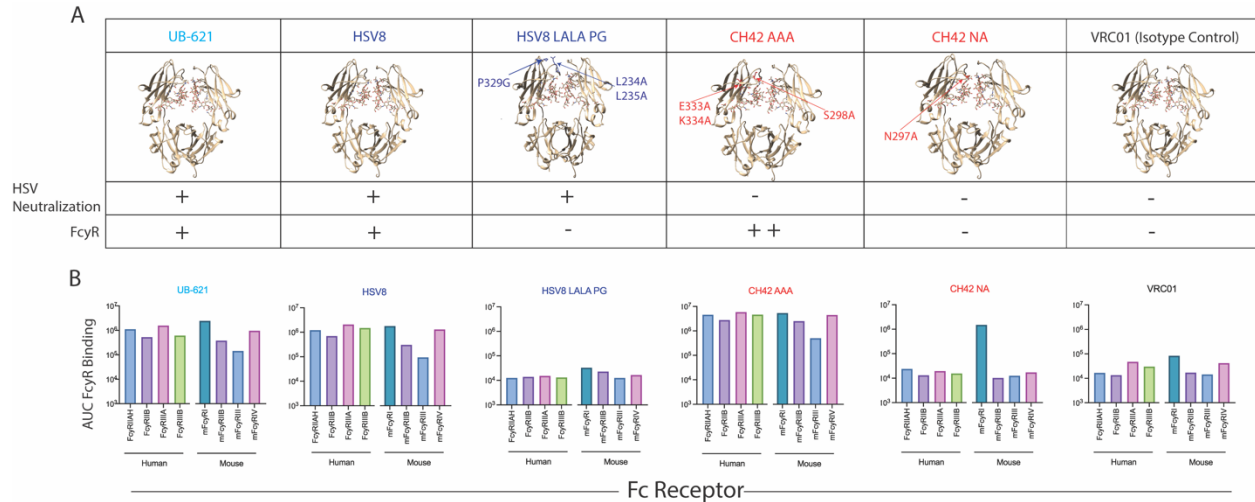


568

569

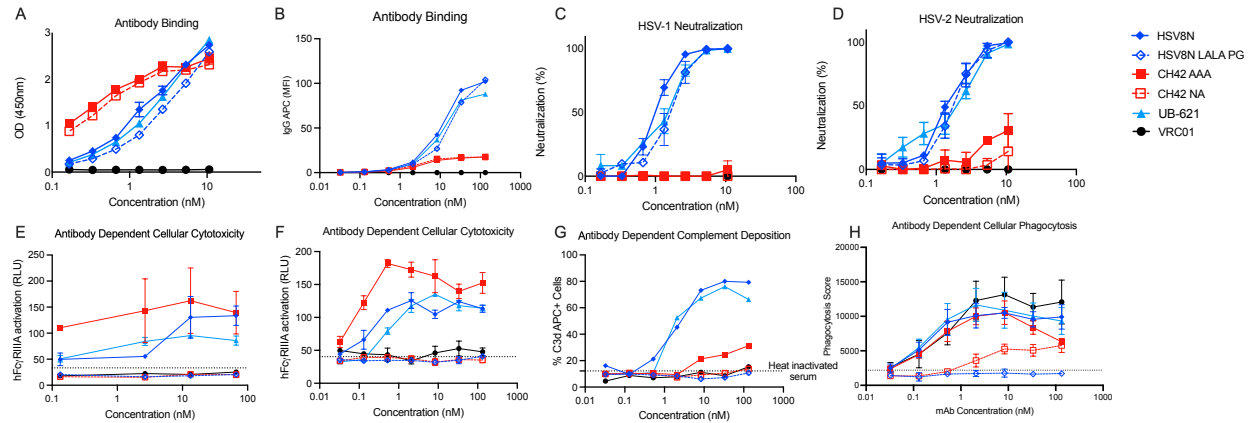
570 **Graphical abstract. Mechanistic dissection of antibody-mediated protection from HSV.**

571 Monoclonal antibodies (mAbs) with varying neutralizing potencies and Fc modifications that
572 impact effector function were evaluated in wildtype (WT) and FcγR^{-/-} mice to define
573 mechanisms of antibody-mediated protection from HSV infection. To model human vulnerability
574 to HSV disease during the neonatal period, neonatal mice were challenged with HSV, treated
575 with mAb, and then assessed for morbidity and mortality. We observed that polyfunctional mAbs
576 provide broader and more potent protection than antibodies with either low neutralization or low
577 effector function. Moreover, while sufficient for protection against HSV-1, neutralization activity
578 alone was unable to protect from HSV-2 infection.



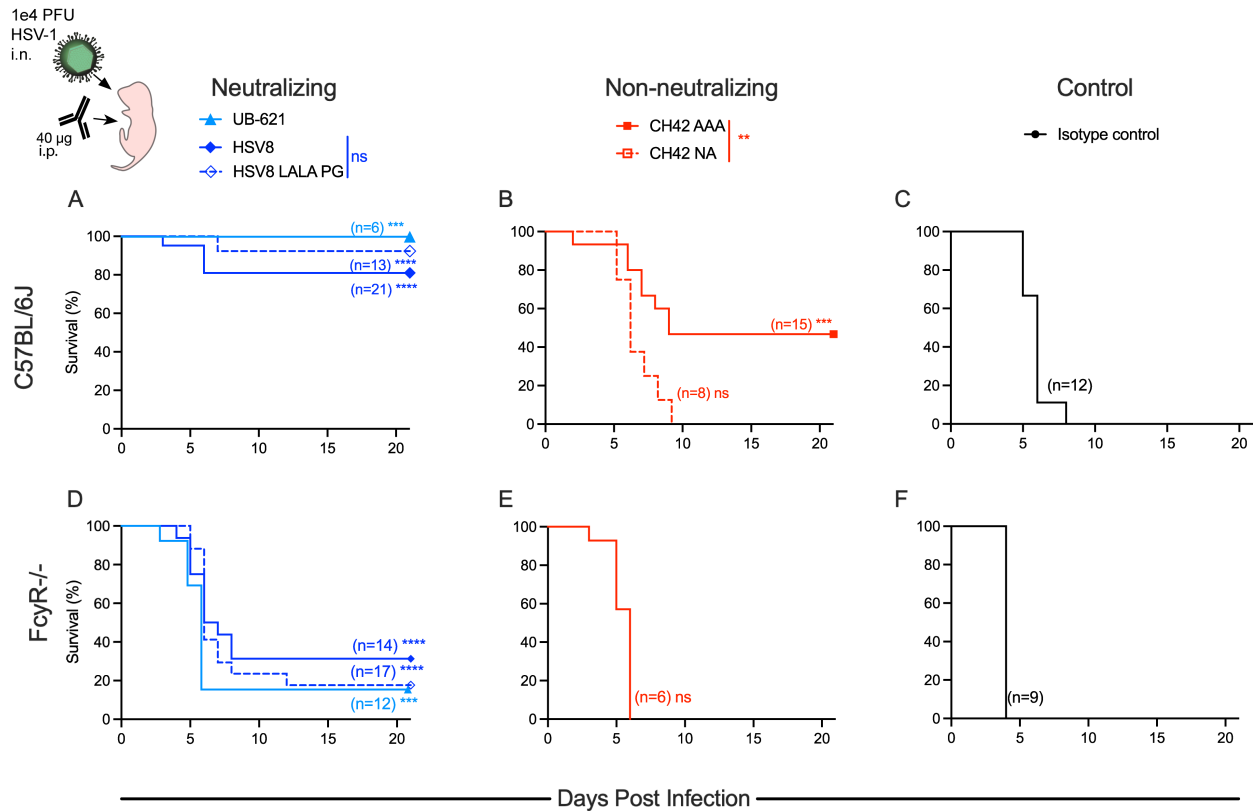
579
580
581
582
583
584
585
586
587
588
589

Figure 1: Biophysical Characterization of HSV gD-specific mAbs. **A.** Visualization of the Fc domains of mAbs used in this study. For reference purposes, mutated positions in the HSV-mAbs are superimposed on the crystal structure of the Fc domain of the HIV-specific mAb b12 (PDB: 1HZH). Reported neutralization potencies of each mAb and the expected ability of each Fc domain to bind FcγRs are indicated. **B.** FcγR binding profiles of the mAbs used in this study. Bar graphs present the area under the curve (AUC) for the binding of each mAb to recombinant human (left) and mouse (right) Fc receptors. Orthologous human and mouse Fc receptors are color matched.



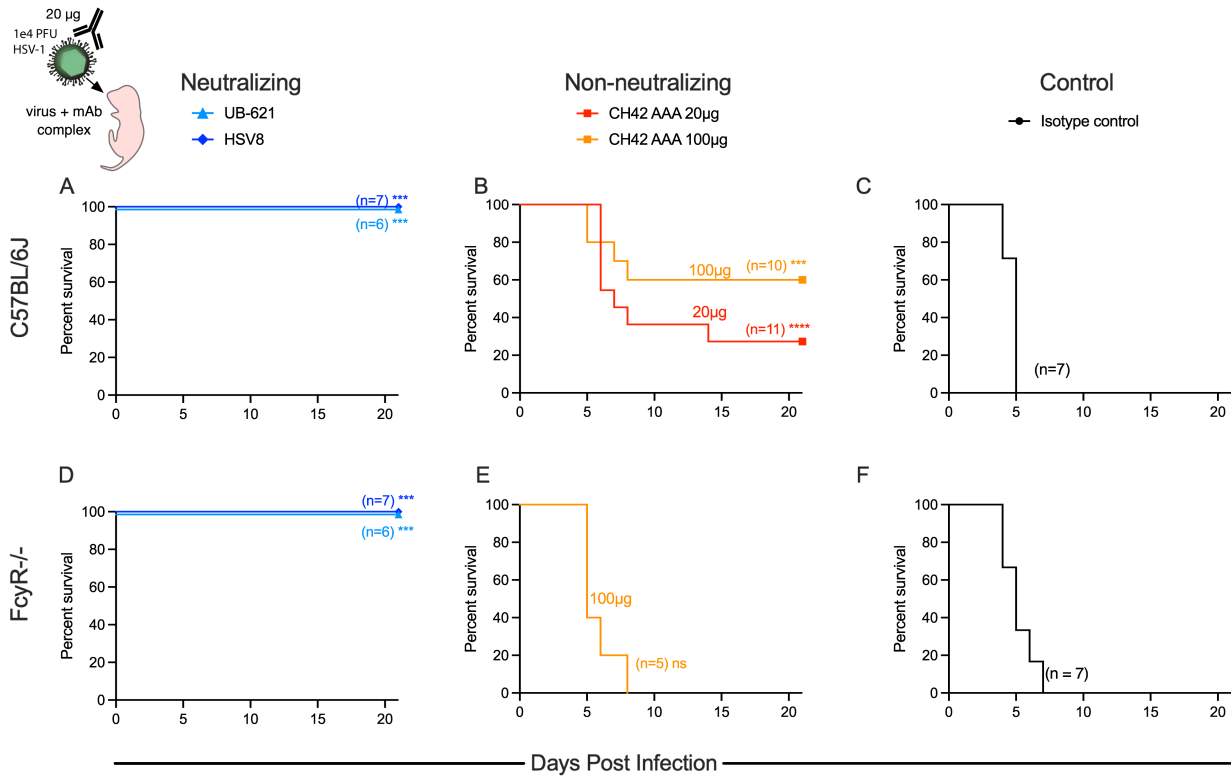
590
591
592
593
594
595
596
597
598
599
600

Figure 2: *In vitro* functional characterization of HSV gD-specific mAbs. A-B. Ability of the HSV gD mAbs to bind recombinant (A) or cell surface-expressed (B) gD via ELISA or flow cytometry, respectively. C-D. Ability of the HSV gD mAbs to neutralize HSV-1 (C) or HSV-2 (D) by plaque reduction assay. E-H. Effector function of HSV gD mAbs, including human FcγRIIIA stimulation of a reporter cell line in the context of antibody-bound gD on a microtiter plate (E), or gD-expressing cells (F) as surrogates for ADCC activity, complement deposition (G), or phagocytosis (H). Error bars represent standard deviation from the mean. OD – optical density, MFI – mean fluorescent intensity, RLU – relative light units, APC – Allophycocyanin.



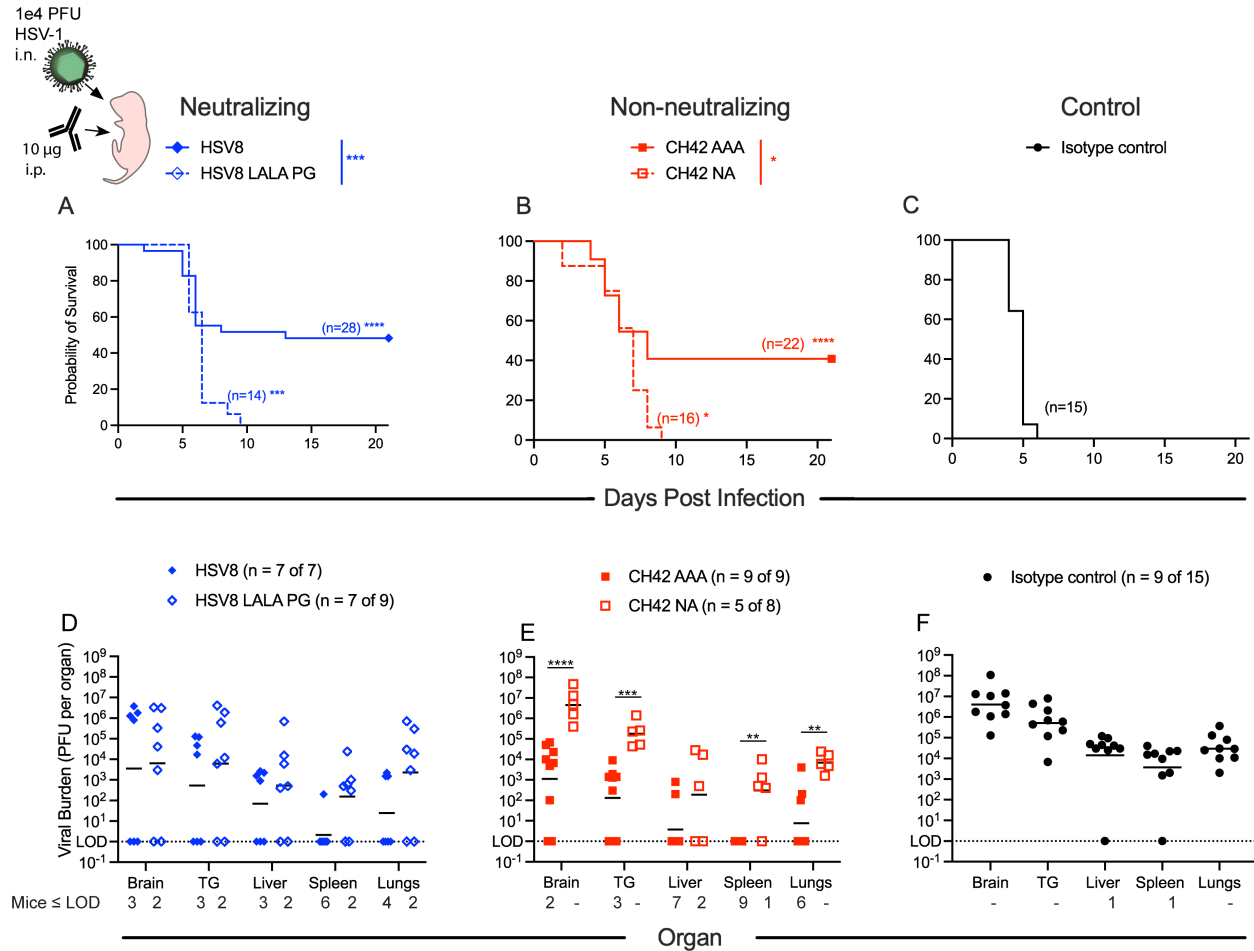
601
602
603
604
605
606
607
608
609
610
611
612
613
614

Figure 3: Both neutralization and effector function contribute to mAb-mediated protection from lethal HSV-1 challenge. Immediately before lethal intranasal (i.n.) challenge with 1×10^4 plaque forming units (PFU) of HSV-1, two-day old pups were administered $40 \mu\text{g}$ of mAb by intraperitoneal (i.p.) injection. **A-C.** Survival of C57BL/6J pups receiving neutralizing mAbs UB-621, HSV8, or HSV8 LALAPG (**A**), non-neutralizing mAbs CH42 AAA or CH42 NA (**B**), or isotype control mAb VRC01 (**C**). **D-F.** Survival of FcyR^{-/-} pups receiving neutralizing (**D**), non-neutralizing (**E**), or isotype control mAb (**F**). Number of mice in each condition and statistical significance as compared to isotype control in matched mouse strain determined by the Log-rank (Mantel-Cox) test (**p < 0.01, ***p < 0.001, ****p < 0.0001) are reported in inset. Significance between HSV8 and HSV8 LALA PG or CH42 AAA and CH42 NA are reported in the above legend as determined by the Log-Rank (Mantel-Cox) test.



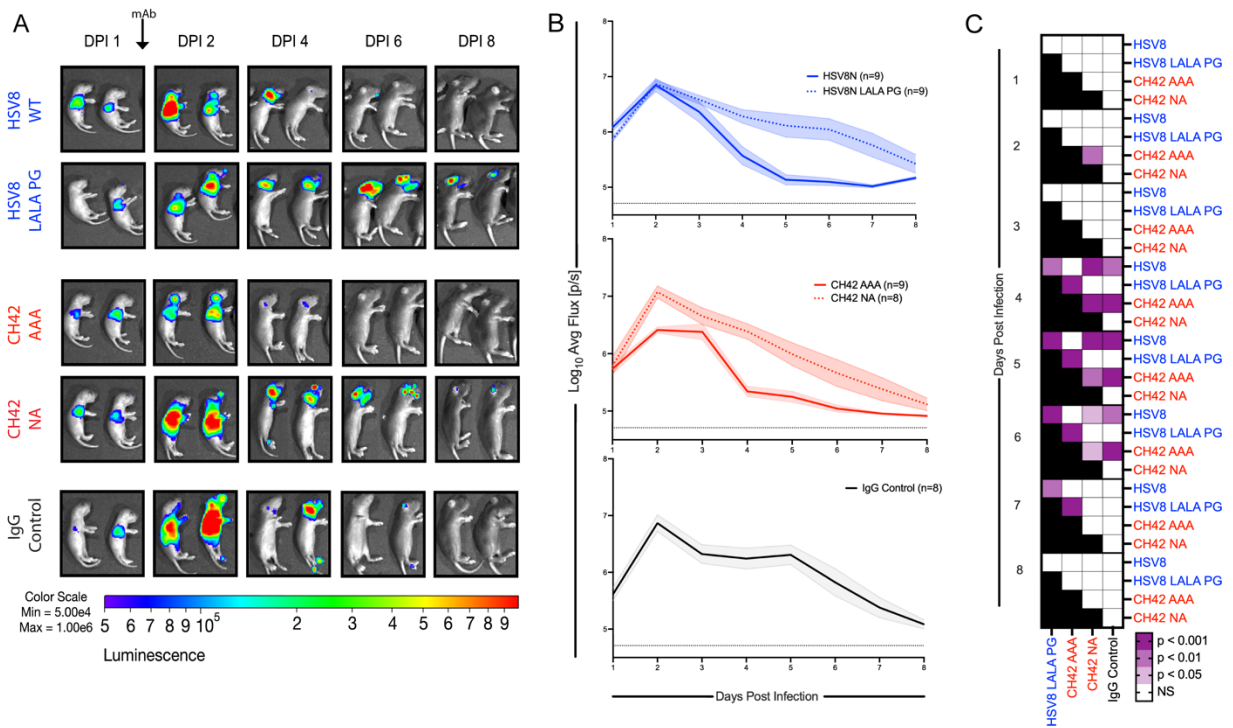
615
616
617
618
619
620
621
622
623
624
625
626
627

Figure 4: Fc functions are protective in the absence of complete viral neutralization. One hour before i.n. challenge of two-day old pups, immune complexes were formed by incubation of 1×10^4 plaque forming units (PFU) of HSV-1 with mAb at 37°C ($20 \mu\text{g}$ unless otherwise noted). **A-C.** Survival of C57BL/6J pups following immune complex challenge with virus opsonized with neutralizing mAbs UB-621 or HSV8 (**A**), non-neutralizing mAb CH42 AAA ($20 \mu\text{g}$ or $100 \mu\text{g}$) (**B**), or isotype control mAb (**C**). **D-F.** Survival of FcyR^{-/-} pups following immune complex challenge with virus opsonized with neutralizing mAbs UB-621 or HSV8 (**D**), non-neutralizing mAb CH42 AAA ($100 \mu\text{g}$) (**E**), and isotype control mAb (**F**). Number of mice in each condition and statistical significance as compared to isotype control in matched mouse strain determined by the Log-rank (Mantel-Cox) test (**p < 0.01, ***p < 0.001, ****p < 0.0001) are reported in inset.



628
629
630
631
632
633
634
635
636
637
638
639
640
641
642
643
644
645
646

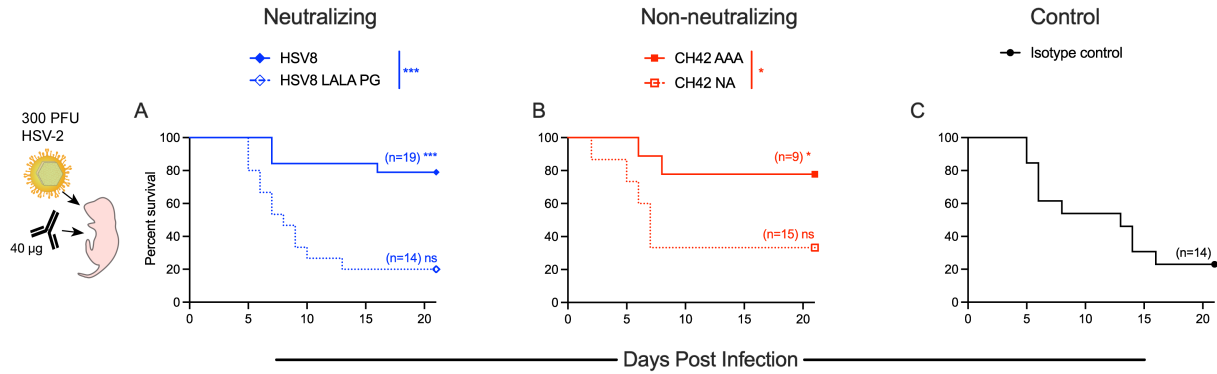
Figure 5: Relative contributions of neutralization and effector functions to protection from lethal challenge depend on antibody dose. Immediately before lethal i.n. challenge with 1×10^4 PFU of HSV-1, two-day old pups were administered $10 \mu\text{g}$ of mAb by i.p. injection. **A-C.** Survival of C57BL/6J pups receiving neutralizing mAb HSV8 or HSV8 LALA PG (**A**), non-neutralizing mAb CH42 AAA or CH42 NA (**B**), or isotype control mAb (**C**). Number of mice in each condition and statistical significance as compared to isotype control determined by the Log-rank (Mantel-Cox) test (* $p < 0.05$, ** $p < 0.01$, *** $p < 0.001$, **** $p < 0.0001$) are reported in inset. Statistical significance between HSV8 and HSV8 LALA PG or CH42 AAA and CH42 NA are reported in the above legend as determined by the Log-rank (Mantel-Cox) test (** $p < 0.01$, *** $p < 0.001$, **** $p < 0.0001$). **D-F.** Viral titers were determined 5 days post infection (DPI). Data are shown as viral burden in perfused organs from surviving pups following $10 \mu\text{g}$ mAb treatment on DPI 0. Statistical significance was determined by 2-way ANOVA with Bonferroni's test for multiple comparisons (** $p < 0.01$, *** $p < 0.001$, **** $p < 0.0001$). Geometric mean of the viral burden in organ type per treatment group is displayed. In legend n = number of pups included in viral titer of the total number of pups treated with mAb to account for pups who died prior to the time point of organ collection.



647
648
649
650
651
652
653
654
655
656
657
658
659

Figure 6: Effector functions accelerate control of viral replication after non-lethal HSV-1 challenge.

One day post i.n. infection with a luciferase-expressing HSV-1, two-day-old pups were administered 10 μ g of mAb i.p. and viral replication, as represented by bioluminescence, was quantified daily. **A**. Representative bioluminescence images of viral infection and replication following mAb treatment are presented for the same two pups over time. **B**. Quantification of virally-derived bioluminescence over time for HSV8 and HSV8 LALA PG (top), CH42 AAA and CH42 NA (middle), and isotype control (bottom). Lines and shaded regions represent the mean luminescence and standard error of the mean across pups (number listed in inset). **C**. Heatmap depicting statistical significance (2-way ANOVA with Tukey's test for multiple comparisons) between groups treated with indicated mAbs over time after infection.



660
661
662
663
664
665
666
667
668
669
670
671

Figure 7: Antibody functions contributing to protection differ between HSV serotypes.

Immediately before lethal i.n. challenge with 300 PFU of HSV-2, two-day old pups were administered 40 µg of mAb by i.p. injection. **A-C**. Survival of C57BL/6J pups receiving neutralizing mAb HSV8 or HSV8 LALAPG (**A**), non-neutralizing mAb CH42 AAA or CH42 NA (**B**), or isotype control mAb (**C**). Number of mice in each condition and statistical significance as compared to isotype control determined by the Log-rank (Mantel-Cox) test (* $p < 0.05$, *** $p < 0.001$) are reported in inset. Statistical significance between HSV8 and HSV8 LALAPG, or CH42 AAA and CH42 NA are reported in the above legend as determined by the Log-rank (Mantel-Cox) test (* $p < 0.05$, *** $p < 0.001$).

672 References

- 673 1. Looker, K. J. *et al.* First estimates of the global and regional incidence of neonatal herpes infection.
674 *Lancet Glob. Health* **5**, e300–e309 (2017).
- 675 2. Whitley, R. *et al.* Predictors of Morbidity and Mortality in Neonates with Herpes Simplex Virus
676 Infections. <http://dx.doi.org/10.1056/NEJM199102143240704>
677 <https://www.nejm.org/doi/10.1056/NEJM199102143240704> (2010)
678 doi:10.1056/NEJM199102143240704.
- 679 3. Melvin, A. J. *et al.* Neonatal Herpes Simplex Virus Infection: Epidemiology and Outcomes in the
680 Modern Era. *J. Pediatr. Infect. Dis. Soc.* **11**, 94–101 (2022).
- 681 4. Kimberlin, D. W. *et al.* Oral Acyclovir Suppression and Neurodevelopment after Neonatal Herpes. *N.*
682 *Engl. J. Med.* **365**, 1284–1292 (2011).
- 683 5. Corey, L. & Wald, A. Maternal and Neonatal Herpes Simplex Virus Infections. *N. Engl. J. Med.* **361**,
684 1376–1385 (2009).
- 685 6. Brown, Z. A. *et al.* Effect of Serologic Status and Cesarean Delivery on Transmission Rates of Herpes
686 Simplex Virus From Mother to Infant. *JAMA* **289**, 203–209 (2003).
- 687 7. Whitley, R. J. *et al.* Changing Presentation of Herpes Simplex Virus Infection in Neonates. *J. Infect. Dis.*
688 **158**, 109–116 (1988).
- 689 8. Kimberlin, D. W. Herpes Simplex Virus Infections of the Newborn. *Semin. Perinatol.* **31**, 19–25 (2007).
- 690 9. Kohl, S. *et al.* Neonatal Antibody-Dependent Cellular Cytotoxic Antibody Levels Are Associated with
691 the Clinical Presentation of Neonatal Herpes Simplex Virus Infection. *J. Infect. Dis.* **160**, 770–776
692 (1989).
- 693 10. Kohl, S. Role of Antibody-Dependent Cellular Cytotoxicity in Neonatal Infection with Herpes Simplex
694 Virus. *Clin. Infect. Dis.* **13**, S950–S952 (1991).
- 695 11. Baron, S., Worthington, M. G., Williams, J. & Gaines, J. W. Postexposure serum prophylaxis of
696 neonatal herpes simplex virus infection of mice. *Nature* **261**, 505–506 (1976).
- 697 12. Balachandran, N., Bacchetti, S. & Rawls, W. E. Protection against lethal challenge of BALB/c mice by
698 passive transfer of monoclonal antibodies to five glycoproteins of herpes simplex virus type 2. *Infect.*
699 *Immun.* **37**, 1132–1137 (1982).
- 700 13. Dix, R. D., Pereira, L. & Baringer, J. R. Use of monoclonal antibody directed against herpes simplex
701 virus glycoproteins to protect mice against acute virus-induced neurological disease. *Infect. Immun.*
702 **34**, 192–199 (1981).
- 703 14. Wang, K. *et al.* Monoclonal Antibodies, Derived from Humans Vaccinated with the RV144 HIV Vaccine
704 Containing the HVEM Binding Domain of Herpes Simplex Virus (HSV) Glycoprotein D, Neutralize HSV
705 Infection, Mediate Antibody-Dependent Cellular Cytotoxicity, and Protect Mice from Ocular
706 Challenge with HSV-1. *J. Virol.* **91**, 10.1128/jvi.00411-17 (2017).
- 707 15. Rector, J. T., Lausch, R. N. & Oakes, J. E. Use of monoclonal antibodies for analysis of antibody-
708 dependent immunity to ocular herpes simplex virus type 1 infection. *Infect. Immun.* **38**, 168–174
709 (1982).
- 710 16. Simmons, A. & Nash, A. Role of antibody in primary and recurrent herpes simplex virus infection. *J.*
711 *Virol.* **53**, 944–8 (1985).

- 712 17. Metcalf, J. F., Koga, J., Chatterjee, S. & Whitley, R. J. Passive immunization with monoclonal
713 antibodies against herpes simplex virus glycoproteins protects mice against herpetic ocular disease.
714 *Curr. Eye Res.* (1987) doi:10.3109/02713688709020086.
- 715 18. Krawczyk, A. *et al.* Impact of Valency of a Glycoprotein B-Specific Monoclonal Antibody on
716 Neutralization of Herpes Simplex Virus. *J. Virol.* **85**, 1793–1803 (2011).
- 717 19. Backes, I. M., Leib, D. A. & Ackerman, M. E. Monoclonal antibody therapy of herpes simplex virus: An
718 opportunity to decrease congenital and perinatal infections. *Front. Immunol.* **13**, 959603 (2022).
- 719 20. Bruhns, P. & Jönsson, F. Mouse and human FcR effector functions. *Immunol. Rev.* **268**, 25–51 (2015).
- 720 21. Goldberg, B. S. *et al.* Revisiting an IgG Fc Loss-of-Function Experiment: the Role of Complement in HIV
721 Broadly Neutralizing Antibody b12 Activity. *mBio* (2021) doi:10.1128/mBio.01743-21.
- 722 22. Gunn, B. M. *et al.* A Fc engineering approach to define functional humoral correlates of immunity
723 against Ebola virus. *Immunity* **54**, 815-828.e5 (2021).
- 724 23. Gunn, B. M. & Alter, G. Modulating Antibody Functionality in Infectious Disease and Vaccination.
725 *Trends Mol. Med.* **22**, 969–982 (2016).
- 726 24. Backes, I. M. *et al.* Maternally transferred monoclonal antibodies protect neonatal mice from herpes
727 simplex virus-induced mortality and morbidity.
728 <http://biorxiv.org/lookup/doi/10.1101/2022.01.12.476098> (2022) doi:10.1101/2022.01.12.476098.
- 729 25. Sanna, P. P. *et al.* Protection of Nude Mice by Passive Immunization with a Type-Common Human
730 Recombinant Monoclonal Antibody against HSV. *Virology* **215**, 101–106 (1996).
- 731 26. Clementi, N. *et al.* Novel therapeutic investigational strategies to treat severe and disseminated HSV
732 infections suggested by a deeper understanding of in vitro virus entry processes. *Drug Discov. Today*
733 **21**, 682–691 (2016).
- 734 27. Shields, R. L. *et al.* High Resolution Mapping of the Binding Site on Human IgG1 for FcγRI, FcγRII,
735 FcγRIII, and FcRn and Design of IgG1 Variants with Improved Binding to the FcγR*. *J. Biol. Chem.* **276**,
736 6591–6604 (2001).
- 737 28. Bailey, M. *et al.* Human antibodies targeting Zika virus NS1 provide protection against disease in a
738 mouse model. *Nat. Commun.* **9**, (2018).
- 739 29. Chao, D. T., Ma, X., Li, O., Park, H. & Law, D. Functional Characterization of N297A, A Murine
740 Surrogate for low-Fc Binding Anti-Human CD3 Antibodies. *Immunol. Invest.* **38**, 76–92 (2009).
- 741 30. Wu, X. *et al.* Rational Design of Envelope Identifies Broadly Neutralizing Human Monoclonal
742 Antibodies to HIV-1. *Science* **329**, 856–861 (2010).
- 743 31. Lo, M. *et al.* Effector-attenuating Substitutions That Maintain Antibody Stability and Reduce Toxicity
744 in Mice *. *J. Biol. Chem.* **292**, 3900–3908 (2017).
- 745 32. Wang, X., Mathieu, M. & Brezski, R. J. IgG Fc engineering to modulate antibody effector functions.
746 *Protein Cell* **9**, 63–73 (2018).
- 747 33. Takai, T., Li, M., Sylvestre, D., Clynes, R. & Ravetch, J. V. FcR gamma chain deletion results in
748 pleiotropic effector cell defects. *Cell* **76**, 519–529 (1994).
- 749 34. Hangartner, L. *et al.* Effector function does not contribute to protection from virus challenge by a
750 highly potent HIV broadly neutralizing antibody in nonhuman primates. *Sci. Transl. Med.* **13**,
751 eabe3349 (2021).
- 752 35. Luker, G. D. *et al.* Noninvasive Bioluminescence Imaging of Herpes Simplex Virus Type 1 Infection and
753 Therapy in Living Mice. *J. Virol.* **76**, 12149–12161 (2002).

- 754 36. Ejercito, P. M., Kieff, E. D. & Roizman, B. Characterization of Herpes Simplex Virus Strains Differing in
755 their Effects on Social Behaviour of Infected Cells. *J. Gen. Virol.* **2**, 357–364 (1968).
- 756 37. Goldberg, B. S. *et al.* Complement contributes to antibody-mediated protection against repeated
757 SHIV challenge. *Proc. Natl. Acad. Sci.* **120**, e2221247120 (2023).
- 758 38. Hessel, A. J. *et al.* Fc receptor but not complement binding is important in antibody protection
759 against HIV. *Nature* **449**, 101–104 (2007).
- 760 39. Spencer, D. A. *et al.* Phagocytosis by an HIV antibody is associated with reduced viremia irrespective
761 of enhanced complement lysis. *Nat. Commun.* **13**, 662 (2022).
- 762 40. Wang, P. *et al.* Quantifying the contribution of Fc-mediated effector functions to the antiviral activity
763 of anti-HIV-1 IgG1 antibodies in vivo. *Proc. Natl. Acad. Sci.* **117**, 18002–18009 (2020).
- 764 41. Asokan, M. *et al.* Fc-mediated effector function contributes to the in vivo antiviral effect of an HIV
765 neutralizing antibody. *Proc. Natl. Acad. Sci.* **117**, 18754–18763 (2020).
- 766 42. Winkler, E. S. *et al.* Human neutralizing antibodies against SARS-CoV-2 require intact Fc effector
767 functions for optimal therapeutic protection. *Cell* **184**, 1804–1820.e16 (2021).
- 768 43. Schäfer, A. *et al.* Antibody potency, effector function, and combinations in protection and therapy for
769 SARS-CoV-2 infection in vivo In vivo efficacy of anti-SARS-CoV-2 antibodies. *J. Exp. Med.* **218**,
770 e20201993 (2020).
- 771 44. Zhang, A. *et al.* Beyond neutralization: Fc-dependent antibody effector functions in SARS-CoV-2
772 infection. *Nat. Rev. Immunol.* **23**, 381–396 (2023).
- 773 45. Goncalvez, A. P., Engle, R. E., St. Claire, M., Purcell, R. H. & Lai, C.-J. Monoclonal antibody-mediated
774 enhancement of dengue virus infection in vitro and in vivo and strategies for prevention. *Proc. Natl.*
775 *Acad. Sci.* **104**, 9422–9427 (2007).
- 776 46. Belshe, R. B. *et al.* Efficacy Results of a Trial of a Herpes Simplex Vaccine. *N. Engl. J. Med.* **366**, 34–43
777 (2012).
- 778 47. Johnston, C., Koelle, D. M. & Wald, A. Current status and prospects for development of an HSV
779 vaccine. *Vaccine* **32**, 1553–1560 (2014).
- 780 48. Aschner, C. B. & Herold, B. C. Alpha herpesvirus Vaccines. *Curr. Issues Mol. Biol.* 469–508 (2021)
781 doi:10.21775/cimb.041.469.
- 782 49. Kohl, S. *et al.* Limited Antibody-Dependent Cellular Cytotoxicity Antibody Response Induced by a
783 Herpes Simplex Virus Type 2 Subunit Vaccine. *J. Infect. Dis.* **181**, 335–339 (2000).
- 784 50. Corey, L. *et al.* Recombinant Glycoprotein Vaccine for the Prevention of Genital HSV-2 Infection Two
785 Randomized Controlled Trials. *JAMA* **282**, 331–340 (1999).
- 786 51. Mahant, A. M. *et al.* Failure of Herpes Simplex Virus Glycoprotein D Antibodies to Elicit Antibody-
787 Dependent Cell-Mediated Cytotoxicity: Implications for Future Vaccines. *J. Infect. Dis.* jiac284 (2022)
788 doi:10.1093/infdis/jiac284.
- 789 52. Belshe, R. B. *et al.* Neutralizing Antibody Kinetics and Immune Protection Against Herpes Simplex
790 Virus 1 Genital Disease in Vaccinated Women. *J. Infect. Dis.* jiac067 (2022) doi:10.1093/infdis/jiac067.
- 791 53. Kuraoka, M. *et al.* A non-neutralizing glycoprotein B monoclonal antibody protects against herpes
792 simplex virus disease in mice. *J. Clin. Invest.* (2022) doi:10.1172/JCI161968.
- 793 54. Dekkers, G. *et al.* Affinity of human IgG subclasses to mouse Fc gamma receptors. *mAbs* **9**, 767–773
794 (2017).

- 795 55. Nimmerjahn, F. & Ravetch, J. V. Divergent Immunoglobulin G Subclass Activity Through Selective Fc
796 Receptor Binding. *Science* **310**, 1510–1512 (2005).
- 797 56. Brown, S. M., Ritchie, D. A. & Subak-Sharpe, J. H. Genetic Studies with Herpes Simplex Virus Type 1.
798 The Isolation of Temperature-sensitive Mutants, their Arrangement into Complementation Groups
799 and Recombination Analysis Leading to a Linkage Map. *J. Gen. Virol.* **18**, 329–346 (1973).
- 800 57. Manivanh, R., Mehrbach, J., Knipe, D. M. & Leib, D. A. Role of Herpes Simplex Virus 1 γ 34.5 in the
801 Regulation of IRF3 Signaling. *J. Virol.* **91**, e01156-17 (2021).
- 802 58. Rader, K. A., Ackland-Berglund, C. E., Miller, J. K., Pepose, J. S. & Leib, D. A. In vivo characterization of
803 site-directed mutations in the promoter of the herpes simplex virus type 1 latency-associated
804 transcripts. *J. Gen. Virol.* **74 (Pt 9)**, 1859–1869 (1993).
- 805 59. Nicola, A. V., Willis, S. H., Naidoo, N. N., Eisenberg, R. J. & Cohen, G. H. Structure-function analysis of
806 soluble forms of herpes simplex virus glycoprotein D. *J. Virol.* **70**, 3815–3822 (1996).
- 807 60. Brown, E. P. *et al.* Multiplexed Fc array for evaluation of antigen-specific antibody effector profiles. *J.*
808 *Immunol. Methods* **443**, 33–44 (2017).
- 809 61. Boesch, A. W. *et al.* Highly parallel characterization of IgG Fc binding interactions. *mAbs* **6**, 915–927
810 (2014).
- 811 62. Butler, S. E. *et al.* Distinct Features and Functions of Systemic and Mucosal Humoral Immunity Among
812 SARS-CoV-2 Convalescent Individuals. *Front. Immunol.* **11**, (2021).
- 813 63. Ackerman, M. E. *et al.* A robust, high-throughput assay to determine the phagocytic activity of clinical
814 antibody samples. *J. Immunol. Methods* **366**, 8–19 (2011).
- 815 64. Rousseaux, M. W. *et al.* TRIM28 regulates the nuclear accumulation and toxicity of both alpha-
816 synuclein and tau. *eLife* **5**, e19809.
- 817
- 818 63. Iida, S. *et al.* Nonfucosylated Therapeutic IgG1 Antibody Can Evade the Inhibitory Effect of Serum
819 Immunoglobulin G on Antibody-Dependent Cellular Cytotoxicity through its High Binding to Fc γ RIIIa.
820 *Clin. Cancer Res.* **12**, 2879–2887 (2006).
- 821 64. Lazar, G. A. *et al.* Engineered antibody Fc variants with enhanced effector function. *Proc. Natl. Acad.*
822 *Sci.* **103**, 4005–4010 (2006).